Orientation in Lipid Bilayers of a Synthetic Peptide Representing the C-Terminus of the A_1 Domain of Shiga Toxin. A Polarized ATR-FTIR Study†

Abdellah Menikh,‡ Mazen T. Saleh,§ Jean Gariépy,§ and Joan M. Boggs*,‡,||

The Research Institute, The Hospital for Sick Children, Toronto, Canada M5G 1X8, Department of Medical Biophysics, University of Toronto and Ontario Cancer Institute, Toronto, Canada M5G 2M9, and Department of Clinical Biochemistry, University of Toronto, Toronto, Canada M5G 1L5

Received April 23, 1997; Revised Manuscript Received October 13, 1997⊗

ABSTRACT: The interaction of a synthetic peptide representing the C-terminal 27 amino acids of the A_1 domain of Shiga toxin (residues 220−246) with acidic phospholipid model membranes was characterized by FTIR spectroscopy. This peptide resembles a signal sequence and may mediate the translocation of the catalytic A_1 chain of Shiga toxin to the cytoplasm following its retrograde transport to the lumenal compartment of the endoplasmic reticulum (ER). At pH 7 and 5, the peptide underwent a conformational change from random coil to α-helix upon addition of negatively charged phospholipids. Examination of the amide II band in the spectrum of the complex at pH 7 and pH 5 showed that in both cases, the N−H groups in the peptide backbone are largely protected from H/D exchange. Using polarized attenuated total reflectance Fourier transform infrared spectroscopy (ATR-FTIR) measurements, the orientation of the α-helical portion of the peptide was found to be almost perpendicular with respect to the membrane plane at pH 7. However, at pH 5.0−5.4, the α-helix axis was preferentially oriented parallel to the membrane plane. The results suggest that at the neutral pH of the ER lumen, the peptide may insert into the membrane, while at the lower pH levels present in earlier endocytic compartments, the peptide would be less likely to traverse the bilayer. In summary, this putative signal peptide may not be able to cause a significant translocation of the A_1 domain of Shiga toxin to the cytosol until it reaches the neutral pH of the ER compartment.

Shiga toxin (ShT)[1] is a protein assembly belonging to a large family of ribosome inactivating proteins. ShT is composed of a single enzymatic subunit (A) and five (B) receptor binding subunits that assemble into a pentamer which binds to Gb_3 (*1, 2*). The A chain possesses a protease-sensitive loop (residues Cys 242 to Cys 261) that can be reduced and cleaved to yield two fragments, an enzymatically active A_1 domain (N-terminus, 27 kDa) and an A_2 fragment (C-terminus, 4 kDa) attached to its B subunit pentamer (*3*). The process by which the catalytic moiety is transferred across a membrane lipid bilayer into the cytosol is not yet understood. The mode of action that has been proposed is linked to its retrograde transport to the endoplasmic reticulum (ER) lumen followed by the retro-translocation of its catalytic A_1 chain to the cytoplasmic side of the ER membrane (*4*).

The C-terminus of the A_1 domain (220−246) contains a series of hydrophobic residues resembling a signal sequence peptide which could be responsible for translocating the A_1 domain across the ER membrane (*5*). The elucidation of the conformational and orientational states of this putative signal peptide in lipid membranes is crucial to reveal the molecular mechanism of the translocation of ShT into the cytoplasm and its toxicity under different environmental conditions.

Therefore, we investigated the interaction with lipid bilayers of a synthetic peptide representing residues 220−246 of ShT containing Ac-RVGRISFGSINAWLGSVALIL-NAHHHA in which Trp was substituted for Ile at position 232 and Ala for Cys at position 242 (*5*).

Circular dichroism measurements have shown that this peptide is a random coil in aqueous solution and largely α-helical when bound to acidic phospholipids or in trifluoroethanol/water mixture. Moreover, a mechanism by which acidic lipid and peptide interact at pH 7 and pH 5 has been proposed based on fluorescence and electron spin resonance measurements of the spin-labeled peptide (*5*). At pH 7, the positively charged N-terminal binds to acidic phospholipid head groups followed by insertion of the hydrophobic core and C-terminus into the membrane. Several lines of evidence support this mechanism. Measurement of the fluorescence of the single tryptophan showed that the protein sensed a more hydrophobic environment upon binding to the membrane. In addition, ESR measurements of peptide spin-labeled at Cys242 indicated that the mobility of the labeled peptide was dramatically restricted in the presence of acidic lipid vesicles and that the label was more accessible to reduction by ascorbic acid trapped inside the vesicles than ascorbic acid added to the outside, suggesting the relocation of the labeled C-terminus to the inside of the bilayer. At

† This study was supported by a postdoctoral fellowship from the Multiple Sclerosis Society of Canada to A.M., and by grants from the Medical Research Council of Canada to J.M.B. and to J.G.

* To whom correspondence should be addressed at The Research Institute, The Hospital for Sick Children, 555 University Ave., Toronto, Ontario, Canada, M5G 1X8. Telephone: (416) 813-5919. Fax: (416) 813-5022. E-mail: jmboggs@sickkids.on.ca.

‡ The Hospital for Sick Children.

§ University of Toronto and Ontario Cancer Institute.

|| University of Toronto.

⊗ Abstract published in *Advance ACS Abstracts,* December 1, 1997.

[1] Abbreviations: FTIR, Fourier transform infrared spectroscopy; ATR, attenuated total reflectance; PG, phosphatidylglycerol; DMPG, dimyristoylphosphatidylglycerol; DPPG, dipalmitoylphosphatidylglycerol; ShT, Shiga toxin; SLT-1, Shiga-like toxin 1.

S0006-2960(97)00944-6 CCC: $14.00

pH 5, however, the spin-label on the peptide was accessible to reduction by ascorbic acid only when the ascorbic acid was added to the outside of the vesicles and not when it was trapped inside the vesicles, suggesting that the labeled positively charged C-terminus of the peptide was located on the outer surface of the membrane along with the positively charged N-terminus.

In light of these results, we have performed spectroscopic studies of the peptide bound to acidic phospholipids at different pH values using conventional transmission FTIR, attenuated total reflection infrared (ATR-FTIR), and polarized ATR-FTIR spectroscopy. These techniques have proven useful for studying the molecular conformation of peptides in lipid bilayer environments. In particular, polarized attenuated total reflection infrared spectroscopy gives information about lipid and protein orientation with respect to the perpendicular axis of the membrane plane (*6*−*8*).

MATERIALS AND METHODS

Materials. Phosphatidylglycerol prepared from phosphatidylcholine (egg PG), dimyristoylphosphatidylglycerol (DMPG), and dipalmitoylphosphatidylglycerol (DPPG) were purchased from Avanti (Alabaster, AL) and used without further purification. D_2O (99.9) was obtained from Merck Sharp & Dohme (Montreal, Canada). The peptide termed $W^{232}A^{242}$ShTA(220−246), representing residues 220−246 of Shiga toxin with two substitutions, I232W and C242A, Ac-RVGRISFGSINAWLGSVALILNAHHHA, was synthesized using standard solid phase techniques and purified as described previously (*5*).

Preparation of Lipid−*Peptide Vesicles.* One milligram of the lipid solution in chloroform/methanol (2:1) was dried under a stream of nitrogen. Residual traces of organic solvent were removed by placing the dried film under vacuum overnight. The lipid film was then dispersed in 0.5 mL of either 2 mM phosphate buffer (pH 7) or 5 mM acetate buffer (pH 3−5) prepared in distilled water. The pH was adjusted with HCl. The samples were heated in a 70 °C water bath and vortexed while the lipid was in the liquid-crystalline phase to ensure complete dispersion. An appropriate amount of dry peptide was then added to these multilamellar vesicles to yield a lipid:peptide molar ratio of 20−25. The dispersion was gently vortexed, lyophilized overnight, and left under vacuum for about 24 h, and then rehydrated with 200 μL of the corresponding buffer in order to ensure retention of the correct pH (*9*). Alternatively, the dispersion was centrifuged in an Eppendorf centrifuge, the supernatant was removed, and the wet pellet was used.

FTIR Spectroscopy. Oriented multilamellar films were prepared either from lipid−peptide solutions in chloroform/methanol (2:1) at a lipid to peptide molar ratio of 20−25 or from the lipid−peptide vesicles prepared at pH 3−7 described above. The ATR-FTIR films were obtained by slowly evaporating 50−60 μL either of the chloroform/methanol solutions or of the preformed lipid−peptide vesicles on one side of an ATR Ge plate (80 × 10 × 4 mm, trapezoid) with a 45° angle of incidence giving 10 internal reflections. The film was dried while moving a Teflon bar back and forth under a stream of purified N_2. When the film is prepared from lipid−peptide solutions in chloroform/methanol, the state of ionization of the peptide is unknown. Since the lipid was provided as the Na^+ salt form, it should be in the ionized form in the dry film. However, when the film is prepared from preformed lipid−peptide vesicles, the states of ionization of the lipid and peptide should be similar to those in the different pH buffers used to prepare the vesicles. A similar approach has been used by others (*8, 10, 11*) in order to vary the state of ionization of proteins. The Ge plate supporting the dry sample was placed in an ATR holder preceded by a rotating KRS-5 (ICR) wire-grid polarizer, and the ATR-FTIR spectra of oriented bilayers were recorded with incident radiation polarized parallel and perpendicular with respect to the normal of the bilayer. For hydration studies, the film was flushed with D_2O vapor in order to eliminate interference from H_2O in the peptide amide I band. The temperature of the sample was altered by a heating block held over the ATR holder, and attached to a controller (Reishert, Austria). In the transmission mode, the hydrated samples were prepared by dropping an aliquot of 10 μL of the preformed lipid−peptide vesicles between two CaF_2 windows, separated by a mylar spacer of 6 μm thickness.

All infrared spectra were measured in a Bruker FTIR Model IFS-48 spectrometer equipped with a germanium-coated KBr beam splitter and DTGS detector. During data acquisition, the spectrometer was continuously purged with high-purity N_2 to eliminate the spectral contribution of atmospheric water. A total of 1000 scans were averaged and Fourier-transformed to yield a spectral resolution of 4 cm^{-1} after triangular apodization. H_2O vapor peaks were subtracted, when necessary, from original spectra interactively. Spectra were smoothed with a factor of 11 using a Savitsky−Golay smoothing procedure, and then corrected for a sloping base line by subtracting a linear base line between 1700 and 1600 cm^{-1}. Spectra were subjected to second-derivative and curve-fitting procedures in order to fit the amide I band in the region 1600−1700 cm^{-1} with a Gaussian band shape, using Spectra Calc (Galactic Industry Corp., Salem, NH). Fitting was judged acceptable when the value of χ^2 was less than 10^{-6}. The results of analysis of the secondary structure of the peptide from several samples were averaged. The results are presented in the text as the mean ± standard deviation.

CD Spectroscopy. An aliquot of the vesicle−peptide mixture was spread on a quartz plate and oriented by a method similar to that of the ATR-FTIR samples. The peptide-free lipid was prepared similarly, and the corresponding spectra were subtracted from the lipid−peptide spectra in order to eliminate light scattering. Hydrated samples were obtained by exposing the dried film to a stream of H_2O vapor. CD spectra were the average of four scans measured on a Jasco J-720 spectropolarimeter by collecting data at 0.1 nm intervals from 240 to 190 nm at room temperature in a nitrogen atmosphere.

Orientation Analysis from ATR-FTIR Dichroism. The electromagnetic field from a propagating light wave penetrating into the Ge−membrane interface exhibits attenuation by the medium. The dichroic ratio (R^{ATR}) was calculated by determining the ratio of either the peak heights or the integrated intensities of the absorption band measured with the incident light polarized parallel and perpendicular with respect to the plane of the bilayer from the following equation (*6*):

$$R^{ATR} = \frac{A_{||}}{A_T} = \frac{E_x^2 k_x + E_z^2 k_z}{E_y^2 k_y}$$

where $A_{||}$ and A_T are the absorbance values measured with parallel and perpendicular polarized light, respectively; E_x, E_y, and E_z are the electric field amplitudes in the x, y, and z direction; and k_x, k_y, and k_z are the integrated absorption coefficients in the x, y, and z direction, respectively. Use of peak heights or integrated intensities gave similar results.

The components of the electric field amplitudes in the film are (*12*)

$$E_x = \frac{2\cos\gamma\,(\sin^2\gamma - n_{21}^2)^{1/2}}{(1-n_{21}^2)^{1/2}[(1+n_{21}^2)\sin^2\gamma - n_{21}^2]^{1/2}}$$

$$E_y = \frac{2\cos\gamma}{(2-n_{12}^2)^{1/2}}$$

$$E_z = \frac{2\cos\gamma\sin\gamma}{(1-n_{21}^2)^{1/2}[(1+n_{21}^2)\sin^2\gamma - n_{21}^2]^{1/2}}$$

where $n_{21} = n_2/n_1$; $n_2 = 1.44$ is the refractive index of the film, and $n_1 = 4$ is the refractive index of the Ge plate; γ (45°) is the angle between the incident electromagnetic field and the normal to the plate. For an axially symmetric molecule whose transition moment is tilted by an angle α with respect to the fiber axis, the components of the integrated absorption coefficient are given by (*13, 14*)

$$k_x = k_y = K\left[\frac{S\sin^2\alpha}{2} + \frac{1-S}{3}\right]$$

$$K_z = K\left[\frac{S\cos^2\alpha}{2} + \frac{1-S}{3}\right]$$

where S is the order parameter and K is a constant. Using these equations, we obtain

$$R = \frac{E_x^2}{E_y^2} + \frac{2E_z^2}{E_y^2}\frac{S(\cos^2\alpha - 1/3)}{S(\sin^2\alpha - 2/3) + 2/3}$$

Accordingly

$$S = \frac{2}{(3\cos^2\alpha - 1)}\frac{E_x^2 + E_z^2 - R^{ATR}E_y^2}{E_x^2 - 2E_z^2 - R^{ATR}E_y^2}$$

If the film refractive index is independent of the wavelength, the above equations can be written in a simplified form, $E_x = 1.398$, $E_y = 1.516$, $E_z = 1.625$, and

$$S = \frac{R^{ATR} - 2}{R^{ATR} + 1.45}\frac{2}{(3\cos^2\alpha - 1)}$$

The order parameter S is related to the fiber axis tilt angle (θ) by the following formula (*12*), assuming a narrow orientation distribution (*15*):

$$S = \frac{3\langle\cos^2\theta\rangle - 1}{2}$$

RESULTS

Conformation of Peptide W^{232}A^{242}ShT(220−246) in Solution. It is well established that the frequency and shape of the amide band depend critically on the secondary structure of a polypeptide chain (*16*). The amide I′ spectral region of the pure peptide W^{232}A^{242}ShTA(220−246) dissolved in D_2O was resolved into six bands (Figure 1) by using the peak positions, obtained from the second-derivative spectra, as input parameters for curve-fitting analysis of the original amide I′ band contour (*17, 18*). The bands centered at 1645 cm^{-1} and at 1641 cm^{-1} are characteristic of peptides which have no well-defined structure (*19*), whereas the band at 1655 cm^{-1} is assigned to α-helical structure (*17, 20*). The components at 1635 and 1625 cm^{-1} are associated with β-sheet structures (*21, 22*). The assignment of the band at 1670 cm^{-1} remains uncertain. Previous studies have correlated this band with unordered structure (*19, 23*) or with the presence of β-turn elements (*21*). However, on the basis of earlier CD results which indicated that the pure peptide in solution had primarily unordered structure with no evidence of α-helix or β-sheet (*5*), we attributed the band at 1670 cm^{-1} to unordered structure.

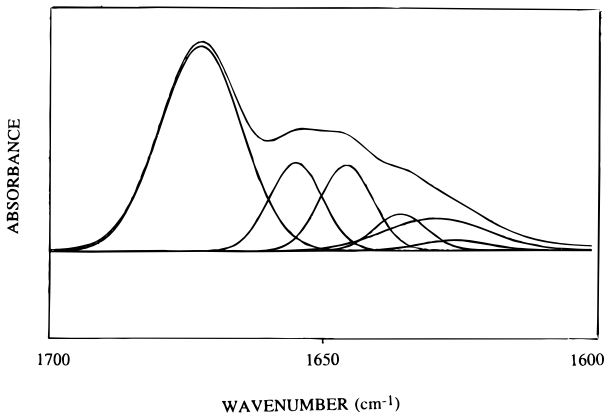

FIGURE 1: Infrared absorbance spectrum in the amide I′ region of the peptide in D_2O. The component bands were obtained by second-derivative resolution and Gaussian curve-fitting analysis (see text).

The results of this analysis reveal that at pH 7 the secondary structure content of the peptide is 12 ± 1% α-helix, 15 ± 3% β-sheet, and 73 ± 5% unordered structure. These values represent the mean and standard deviations of results on several different samples. In contrast to our earlier CD results which detected only random structure, the FTIR data show clearly that, even in the absence of acidic phospholipid, the secondary structure contains a proportion of α-helix and β-sheet. Using the Chou and Fasman (*24*) method of prediction, we found that the most probable sites of the α-helical and β-sheet structures are, respectively, between residues 227−234 and 220−226 in the peptide backbone, in agreement with those determined from the X-ray crystallography study of Shiga toxin (*2*). These segments satisfy all predictive conditions including $[P_\alpha] = 1.06$, $[P_\alpha] > [P_\beta]$ for the α-helix and $[P_\beta] = 1.18$, $[P_\beta] > [P_\alpha]$ for the β-sheet.

When the solution of the peptide was dried into a film on the ATR-Ge plate, analysis of the FTIR spectrum showed that the structure was 9% α-helix, 59% β-sheet, and 31% unordered. This indicates that most of the free peptide aggregates during the drying process.

Peptide Secondary Structure in Phospholipid Bilayers and pH Dependence. The amide I region of ATR-FTIR spectra of dry films of the peptide−DPPG complex at three different pH values is shown in Figure 2. When the film is dried

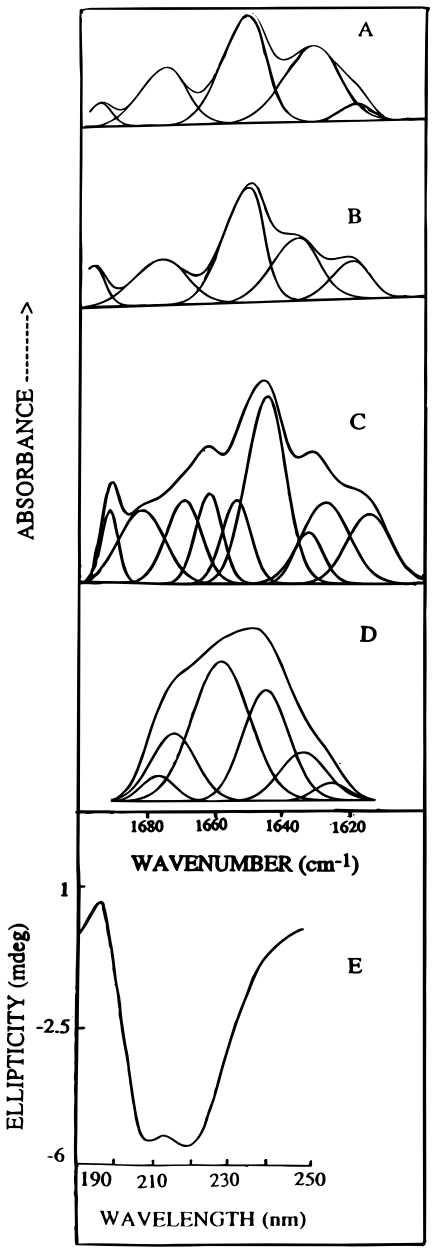

FIGURE 2: Secondary structure determination of peptide−DPPG film dried from (A) 5 mM acetate buffer, pH 5, (B) 2 mM phosphate buffer, pH 7, and (C) 5 mM acetate buffer, pH 3, on a FTIR-ATR Ge plate. (D) Infrared absorbance spectrum in the amide I′ region of the peptide−DPPG dispersion in D_2O (neutral pH). (E) Circular dichroism spectrum in the far-ultraviolet region of a hydrated peptide−DPPG film. Curve-fitting analysis was carried out as described under Materials and Methods.

from pH 7 buffer, the lipid phosphate should be ionized since the pK_a of the phosphate of DPPG is below pH 4 (*25*). The peptide histidines should be neutral, the arginines should be protonated, and the C-terminal carboxyl should be ionized. At pH 5, the lipid should still be ionized and the peptide histidines should be protonated. At pH 3, the lipid phosphate and the peptide C-terminal carboxyl should be protonated. We could not detect the state of ionization of the His from the FTIR spectra. However, the state of ionization of the peptide carboxyl and the lipid phosphate could be determined from the ATR-FTIR spectra. At pH 3, the spectrum of the DPPG−peptide complex had a significant band at 1692 cm^{-1} (Figure 2C), characteristic of a protonated carboxyl group (*26*). This band partially overlaps with an amide I band at

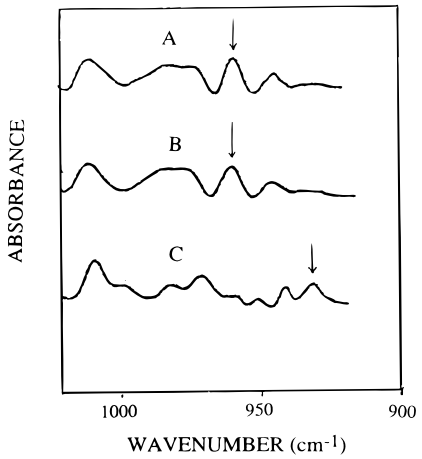

FIGURE 3: ATR-FTIR spectra of the phosphate stretching modes of DPPG−peptide films dried from (A) 2 mM phosphate buffer, pH 7; (B) 5 mM sodium acetate buffer, pH 5.4; and (C) 5 mM sodium acetate buffer, pH 3. Bands due to the P−OH stretching vibration at 932 cm^{-1} and the P−O^- stretching vibration at 960 cm^{-1} are indicated by arrows.

1696 cm^{-1} attributed to an antiparallel β-sheet, but the band intensity at 1692 cm^{-1} was greatly diminished for the DPPG−peptide complex at pH 5 and 7 (Figure 2A,B, respectively), consistent with ionization of the carboxyl above pH 5. This indicates that the ionization state of the peptide in the dry film was dependent on the pH of the original dispersions. The ionization state of the lipid was also dependent on the pH of the original dispersions as shown by the phosphate stretching region from 1000 to 900 cm^{-1} of the lipid−peptide film in Figure 3. Binding of the peptide did not alter the frequency of the phosphate group. At pH 3, a band occurs at 932 cm^{-1} due to the P−OH stretching mode of the protonated phosphate (*27*, *28*). At pH 5.4−7, a small but well-resolved band appeared at 960 cm^{-1} due to the ionized P−O^- group. This is accompanied by a drastic decrease of the stretching P-OH vibration at 932 cm^{-1}. At pH 5, the phosphate appeared to be partially protonated (not shown), but at pH 5.4 it was completely ionized.

For the dry DPPG−peptide film prepared from pH 7 buffer, curve-fitting analysis of the second-derivative spectrum gave five bands at 1696, 1675, 1652, 1632, and 1616 cm^{-1}, assigned to protein structure (*20*) (Figure 2B). The peak at 1632 cm^{-1} has been attributed to an extended β-sheet structure by many investigators (*29*, *30*), while the band at 1616 cm^{-1} is assigned to strongly intermolecularly hydrogen-bonded β-sheet (*20*, *31*). Nevertheless, the assignment of the band located at 1675 cm^{-1} is less obvious. Previously, it has been attributed to β-sheet (*17*). However, wheat ω-gliadins with a high content of β-turns absorb around 1675 cm^{-1} (*32*). Therefore, we have attributed the band at 1675 cm^{-1} to β-turn. The band at 1652 cm^{-1} found in dried films may originate from either α-helix or unordered structure (*33*). However, the frequency of the amide I (C═O) region was unaffected by D_2O vapor, indicating that the peptide has only ordered structure in which all peptide bonds are involved in hydrogen bonding. Furthermore, the far-UV region of the CD spectrum of an oriented film shows double minima at 208 and 222 nm (Figure 2E), characteristic of α-helical structure. Therefore, we assigned the band at 1652 cm^{-1} to α-helix (*17*, *20*, *31*). The weak component at 1696 cm^{-1} probably reflects a high-frequency vibration of an antiparallel β-sheet (*34*, *35*). This curve-fitting analysis revealed that

the peptide bound to DPPG contained 46 ± 2% α-helix, 24 ± 3% *β*-turn, and 29 ± 1% *β*-sheet at pH 7 (Figure 2B).

The infrared spectrum in the transmission mode of hydrated lipid−peptide dispersions in D_2O (neutral pH) was also investigated (Figure 2D); the peptide secondary structure in hydrated bilayers contained 41 ± 4% α-helix, 14 ± 1% *β*-sheet, 19 ± 2% *β*-turn, and 25 ± 4% random coil. The α-helix proportion determined from the transmission mode is compatible with that obtained from the CD spectra of hydrated samples shown here and reported previously (45−50%) (*5*), and from the ATR-FTIR spectra of dry films. Since only 50% of the peptide was found to bind to DMPG small unilamellar vesicles in the earlier study (*5*), this result suggests that the membrane-bound peptide is significantly α-helical.

At pH 5−5.4, no significant changes in the amide I contour were observed for the ATR-FTIR dry films (Figure 2A). The secondary structure was minimally affected by a decrease in pH, except for a slight increase of the *β*-sheet. At pH 5, the peptide contained 42 ± 4% α-helix, 35 ± 2% *β*-sheet, and 23 ± 1% *β*-turn. At pH 5.4, similar values were obtained. However, when the pH was dropped to 3, the peptide structure changed to 44% unordered structure, 36% *β*-sheet, and 21% α-helix (Figure 2C). The large decrease in α-helical structure and increase in unordered structure reflect its decreased interaction with the protonated DPPG at pH 3.

Further insight into the conformation of the peptide in DPPG may be obtained by following the intensity of the amide II absorption peak [δ(N−H)] at around 1547 cm^{-1}, after exposure of the dry film to D_2O vapor. This intensity reflects the rate of hydrogen/deuterium exchange of the NH amide groups of the peptide. No appreciable loss in peak absorption of the amide II band was observed at pH 5−7, at least in the first 120 min of incubation with D_2O (not shown). This finding indicates that the N−H groups either are involved in intramolecular hydrogen bonding in α-helical or *β*-structure and/or are embedded in the lipid bilayer.

Effect of the Peptide on the Lipid Acyl Chains. The effect of the peptide on the lipid fatty acids can be determined by monitoring the frequency of the C−H stretching vibrations. Only the symmetric stretching band was analyzed because the peptide bands do not interfere with this spectral region (*36*). In an ordered phase at room temperature, the symmetric stretching vibration of a dry film of pure DPPG at neutral pH and pH 5 was located at 2848 cm^{-1}, a frequency characteristic of highly ordered fatty acid. However, in the presence of the peptide, this band shifted upward to 2850 cm^{-1}, indicating significant disordering of the lipid fatty acid. Elevation of the temperature to 70 °C, above the phase transition temperature of the lipid, which was 63 °C for the dry film, shifted the symmetric stretching vibration further to 2852 cm^{-1}, a frequency identical to that of lipid alone at this temperature. Identical results were observed at pH 7 and 5. These results indicate that the peptide disorders the lipid chains in the ordered state but has no effect on chain order in the fluid phase.

Orientation Study of the Peptide in Phospholipid Bilayers. Both FTIR and CD results demonstrated the prominent feature of α-helical structure of the peptide in the presence of negatively charged phospholipid. On the basis of accessibility of the spin-labeled peptide to ascorbic acid in our earlier study (*5*), the location and orientation of the peptide in the bilayer have been proposed to be perpendicular to the bilayer at pH 7 and parallel at pH 5. In this study, we have established that the N−H groups of the peptide backbone were resistant to proton/deuterium exchange, indicating that the peptide N−H groups may be protected by the lipid bilayer at both pH values. Alternatively, the resistance to exchange may be due to stable forms of secondary structure. Using polarized ATR-IR spectroscopy, it is possible to determine the orientation of the α-helical segments with respect to the perpendicular to the plane of the bilayer (*37*, *38*).

First, the orientation of the lipid chains of a dry film of the pure lipid was determined from the CH_2 symmetric stretching vibration at 2848 cm^{-1} in the ATR-FTIR absorbance spectrum using perpendicular and parallel polarized light. The experimental average dichroic ratio was 1.08. Assuming that the transition dipole moment of the symmetric CH_2 stretching vibration is perpendicular to the molecular axis (*6*), the resulting calculated order parameter S of the acyl chains was 0.72 and the average tilt angle θ of the lipid CH_2 axis was 26°, in agreement with previously observed results for well-ordered fatty acid chains in the gel phase (*28*, *39*).

Upon lipid−peptide complexation at pH 7, the dichroic ratio for the CH_2 symmetric stretching vibration of a dry film at 2850 cm^{-1} increased to 1.17, giving an order parameter of 0.63 and an average tilt angle of 33° for the lipid chain axis. This change in the tilt angle indicates that a number of gauche conformers have been introduced into the system and/or a change in the average orientation of the hydrocarbon chain axis occurred without deformation of the lipid fatty acid. The fact that the peptide increased the frequency of the CH_2 symmetric stretching vibration indicates that it increased the gauche content. The average dichroic ratio obtained for the peptide α-helix band at 1652 cm^{-1} using parallel and perpendicular polarized light was found to be 3.5 (Figure 4). The order parameter was calculated by assuming values of 22° (*40*) and 39° (*41*) for the angle α of the dipole moment with respect to the α-helix axis. This result gave values for S of 0.38 and 0.74, respectively, corresponding to values for θ of 39° and 24°, respectively, suggesting that the peptide inserts into the lipid bilayer with its α-helix axis on average almost parallel to the fatty acyl chains. Similar results were found when a DMPG−peptide mixture was dried from chloroform/methanol on the ATR-Ge plate. The frequency of the C−H stretching vibrations indicated that DMPG was in the gel state. The tilt angle of the DMPG acyl chains was 26°, and that of the peptide was 42°−29°.

At pH 5, the polarized ATR-FTIR spectra of the dry film of the complex of the peptide with DPPG gave an average dichroic ratio $R = 1.12$ for the amide I α-helix band at 1652 cm^{-1} and $R = 1.16$ for the symmetric stretching vibration of the lipid CH_2 groups, corresponding to an order parameter of −0.43 and a tilt angle of the α-helix axis of 77° (for a value of $\alpha = 22°$) and an order parameter for the fatty acid chain axis of 0.64 and a tilt angle of 29°, with respect to the normal of the bilayer. It is worth noting that at $\alpha = 39°$, the α-helix order parameter ($S = -0.8$) is less than the physically acceptable value ($S = -0.5$). Since the lipid was partially protonated at pH 5, this experiment was repeated at pH 5.4 where it was completely ionized. At pH 5.4, the dichroic ratio for the amide I α-helical band was 1.23, giving

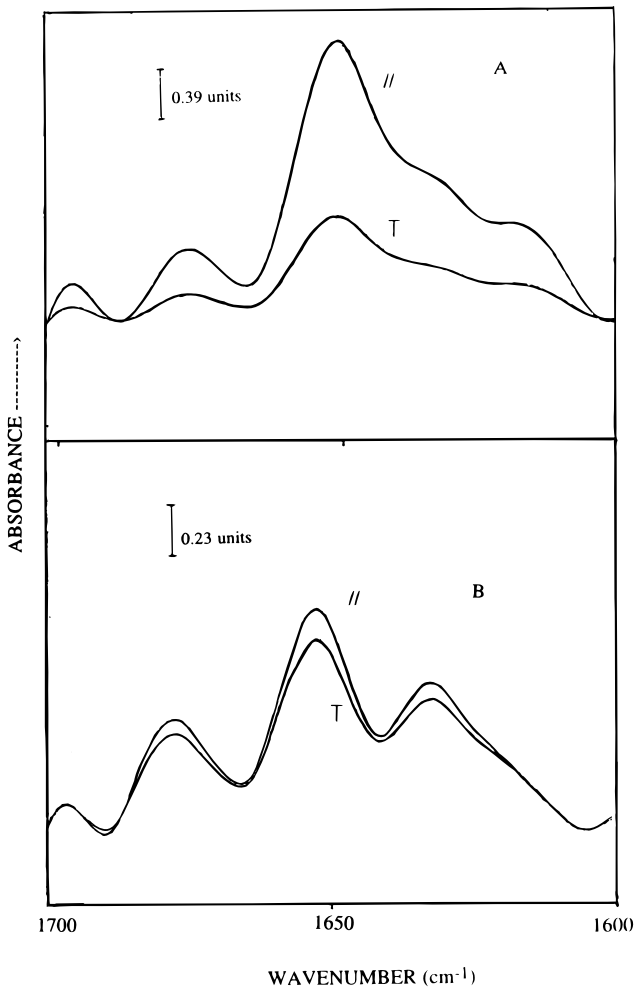

FIGURE 4: Parallel (||) and perpendicular (T) polarized ATR-FTIR absorbance spectra in the amide I region between 1700 and 1600 cm^{-1} of DPPG−peptide films dried from (A) 2 mM phosphate buffer, pH 7, and (B) 5 mM sodium acetate buffer, pH 5.4.

an order parameter of −0.36 corresponding to a tilt angle of 71° (for $\alpha = 22°$). This finding implies that at pH 5−5.4, the average orientation of the α-helix is essentially parallel to the membrane plane (*14*), in agreement with our previous model in which we suggested that the positively charged N- and C-termini interact with the lipid head groups, and the hydrophobic core of the peptide inserts into the lipid bilayer in the interfacial region, parallel to the surface (*5*).

Flushing the samples with D_2O vapor had little effect on the lipid chain orientation as judged by comparison of the value of the tilt angle for dry and hydrated samples, indicating that the lipid film was still well oriented after hydration. However, at pH 7 the dichroic ratio of the α-helix decreased to 2.17 giving an order parameter close to 0. This corresponds either to an orientational distribution of the α-helix around an angle of 52−50°, which is close to the magic angle of 54.7°, or to random orientation of the α-helix. At pH 5, the dichroic ratio for the peptide increased to 2.16, giving a similar order parameter close to 0. Therefore, we cannot conclude whether the observed changes of hydration are a result of uniform tilting of the α-helix axis at an average angle of about 52° or random orientation of the peptide.

Heating the dried pH 7 sample to 70 °C, above the phase transition temperature of the lipid at 63 °C, caused a slight increase in the proportion of α-helix at the expense of β-sheet, an increase in the tilt angle of the hydrocarbon chains from 26° to 51°, and a decrease in the order parameter of the α-helix axis to approximately 0. Similar results were also observed with egg PG at room temperature when the peptide was mixed with lipid in chloroform/methanol, and dried on the Ge plate, or when the film was prepared from preformed egg PG/peptide dispersions at pH 7. Thus, it cannot be determined if the peptide is uniformly tilted in the lipid fluid phase at an average angle of about 52° or if it has become randomly oriented.

DISCUSSION

This paper reports structural and orientational studies of a synthetic peptide corresponding to the C-terminus of the A_1 domain of Shiga toxin in lipid bilayers using FTIR spectroscopy. The analysis of secondary structure from FTIR data shows that the peptide in solution adopts a random structure with a small contribution of α-helix and β-sheet. Secondary structure predictions suggest that residues between 227−334 and 220−226 are the most likely sites of α-helix and β- sheet formation, respectively, in agreement with the structure of these segments in the X-ray crystal structure of Shiga toxin (*2*).

Upon complexation with DPPG at pH 7, the FTIR spectrum of a dry film indicated that the peptide acquired 46% α-helix, 24% β-turn, and 29% β-sheet structure. In lipid dispersions in the presence of water, the peptide had a similar amount of α-helical and β-turn structure but less β-sheet structure than the dry film, and 25% unordered structure. However, in a dry film in the absence of lipid, the peptide had 59% β-sheet structure, 31% unordered structure, and only 9% α-helical structure. Since our earlier study with DMPG vesicles (*5*) showed that only about half of the peptide was bound to the lipid, this result indicates that the membrane-bound peptide, especially the hydrophobic midsection, is significantly α-helical as concluded earlier from CD measurements, while the unbound peptide and perhaps also the ends of the peptide contribute to the unordered structure in the spectra of hydrated dispersions. Similarly in the dry film, the unbound peptide must contribute to the β-structure of the dry DPPG−peptide sample. Since the unbound peptide cannot remain in solution after drying the lipid−peptide film, it may aggregate at the surface of the bilayers in the form of β-sheet structure, thus accounting for the increase in β-sheet structure and the elimination of random structure on drying the sample. The secondary structure was not affected significantly by lowering the pH to 5, suggesting that about half of the peptide is still associated with the lipid bilayer in a nonaggregated, mostly α-helical form. At pH 3, where the peptide is not likely to bind to the protonated lipid in the dry film, it had mostly β-sheet and random structure.

The absence of rapid H/D exchange of the amide N−H in peptide−lipid films exposed to D_2O vapor indicates that the N−H groups in the peptide backbone are locked in hydrogen bonds and/or embedded in the bilayer, at both pH 7 and pH 5. These observations were corroborated by the absence of the unfolded state in the dry peptide−lipid films, which would have readily favored the exchange of N−H protons with aqueous deuterons.

The most significant result of the present work is the determination of the average orientation of the α-helical portion of the peptide in the phospholipid bilayer. Although

the peptide may have a broader distribution of orientations than indicated by the calculated tilt angle, the large difference in dichroic ratio for the peptide at pH 7 and 5 in dry films indicates that there is a large difference in its average orientation at these pH values. Thus, the ATR-FTIR results indicate that the α-helix binds nearly parallel to the plane of the DPPG bilayer at pH 5−5.4 and inserts nearly perpendicular to it at pH 7. This conclusion could be drawn only from dry films and from the ordered state of DPPG or DMPG. In the fluid state of DPPG or in egg PG, the lipid chains and the peptide may have been either more randomly oriented or all tilted at an average angle of about 52°, close to the magic angle. Similarly, hydration of DPPG films in the gel state at pH 5−7 either caused a change in the tilt angle of the peptide to about 52° or caused its orientation to become more random.

Thus, for dry films, the topography of the peptide in the bilayer is clearly different at pH 7 and 5. At pH 7, the hydrophobic peptide, positively charged only near the N-terminal end, is able to insert into the bilayer and orient parallel to the acyl chains. At pH 5, protonation of the three histidines at the C-terminal end prevents this insertion, and the peptide is bound to the surface of the bilayer, nearly parallel to it, with the hydrophobic midsection possibly dipping into the bilayer. In spite of the fact that a similar amount of peptide is bound to acidic lipid bilayers and that it acquires a similar amount of α-helical structure at pH 7 and 5, the lack of insertion of the peptide into the bilayer at pH 5 indicates that binding and α-helicity alone are not sufficient to induce insertion.

The peptide caused a similar reduction of the lipid hydrocarbon chain order in the ordered state at both pH 7 and pH 5, but had no effect in the fluid state. Thus, the inserted transmembrane peptide has a similar effect on the lipid chains as the peptide adsorbed to the surface of the bilayer. This may be coincidental. The decrease in order in the ordered state caused by the peptide at pH 7 is similar to the effect of the peptide Lys_2-Gly-Leu_{24}-Lys_2-Ala-amide in saturated forms of phosphatidylcholine which form bilayers thicker than the length of the hydrophobic α-helical portion of the peptide (*42*). Thus, the lipid becomes disordered in order to accommodate to the shorter length of the peptide. The hydrophobic portion of $W^{232}A^{242}$ShTA-(220−246) may also be too short for a DPPG bilayer. If only the midsection made up of 19 hydrophobic or neutral residues (224−242) forms an α-helix, the length would be 28.5 Å (at 1.5 Å per residue) while the thickness of the acyl chain region of a DPPG ordered phase bilayer would be about 39.4 Å (*42*). The fluid phase with a hydrophobic thickness of 26.3 Å could better accommodate the hydrophobic portion of this peptide, and thus the gauche content of the lipid chains is not affected in the fluid phase. At pH 5, the peptide may disorder the lipid ordered phase by lying on the surface with its hydrophobic side chains dipping into the bilayer.

Upon hydration, the degree of peptide orientation clearly decreases at both pH 7 and pH 5. However, the fact that the order parameter is close to 0 at both pH values makes it impossible to detect differences in the topography of the peptide at these pH values by ATR-FTIR, since either random orientation, orientation at a fixed angle of about 52°, or other distributions of orientations of the α-helix could result in an order parameter of 0.

The orientation of melittin and alamethicin in lipid bilayers has been found to change dramatically when the degree of hydration was changed (*14, 43*). However, in those cases, the order parameter was not close to 0 in either the dry or the hydrated states, allowing conclusions to be drawn concerning orientation in both cases. In the case of $W^{232}A^{242}$ShTA(220−246), its orientation in hydrated films is ambiguous, but the data do not rule out similar relative differences in topography at pH 5 and 7 as found for dry films. For example, at pH 7, in hydrated films the peptide could span the bilayer with an end on each side of the bilayer but be tilted at an angle of about 52° or at a range of angles. At pH 5, both ends of the peptide could be anchored at the bilayer surface on one side of the bilayer with the hydrophobic midsection dipping further into the bilayer than in the dry film. Thus, each half from the end to the middle could be oriented at an angle of 52° with respect to the bilayer normal without spanning the bilayer. Other models are also consistent with the data.

Alternatively, the ATR-FTIR results may indicate a similar orientation in hydrated films at pH 7 and 5. However, this would not be consistent with our earlier results on the peptide bound to lipid vesicles in the presence of excess water at pH 7 and 5 (Saleh et al., 1996). These results showed that the C-terminal end of the peptide was much more exposed on the outside of the vesicles at pH 5 than at pH 7 and that it was much more exposed on the inside of the vesicles at pH 7 than at pH 5. Since the N-terminal end is positively charged in both cases, these results suggested an orientation of the peptide perpendicular to the bilayer at pH 7, with the C-terminal end on the inside of the vesicles, and an orientation parallel to the bilayer at pH 5. The ATR-FTIR results on dry films presented in this study show that under some conditions at least, the peptide orientation clearly does depend on pH in this manner. The dry films were prepared from lipid vesicles to which the peptide in solution at different pH values was added. The pH dependence of the results on dry films indicates that the peptide in solution must have inserted into the bilayer in a pH-dependent way. This indicates a greater tendency of the C-terminal end of the peptide to insert into the bilayer at pH 7 than at pH 5. This greater tendency should prevail in hydrated bilayers, although increased disorder makes it impossible for us to detect it by ATR-FTIR.

The results on dry films support the hypothesis that the hydrophobic domain at the C-terminus of the A_1 domain of ShT may be able to act as a signal peptide which could promote the translocation of the A_1 domain from the lumen of the ER to the cytosol. It might do so by making use of components of the protein translocation machinery of the ER normally used to translocate newly synthesized proteins in the reverse direction. ShT is similar to Shiga-like toxin 1 (SLT-1) (one amino acid difference) and is homologous to ricin toxin. These toxins behave differently from diphtheria toxin with a pH-sensitive hydrophobic domain which becomes exposed in a low-pH compartment (reviewed in *44, 45*). Thus, lysosomotrophic agents such as NH_4Cl protect cells from diphtheria toxin. In contrast, the conformation of SLT-1 is not pH-sensitive (*46*), and NH_4Cl does not protect cells against the toxin (*47*). A signal peptide which becomes exposed after proteolytic processing would allow ShT and similar toxins to translocate across the ER. Although the ShT peptide orientation in hydrated bilayers

may not be as distinctly different as in dry films, its tendency to orient perpendicular to the bilayer at pH 7 would stimulate translocation of the toxin at this pH. The results on dry films indicate a decreased tendency for it to be oriented perpendicular to the bilayer at pH 5, which would inhibit translocation of the toxin at this pH value. Thus, in the case of ShT, the pH dependence of insertion of the signal peptide into the bilayer found for dry films suggests that membrane insertion of the A_1 domain in earlier lower pH endosomal compartments would be retarded until the toxin reached the higher pH of the ER.

Ricin toxin also has a hydrophobic domain near the C-terminus of its catalytically active A chain. Dissociation of the ricin A chain from the B chain is thought to occur in the ER lumen and would cause exposure of its hydrophobic domain (*48*). Mutations in the hydrophobic domain of ricin decreased the toxicity of the toxin but did not affect its enzymatic activity (*49*), suggesting that they may have affected its ability to translocate to the cytosol. A fusion protein containing this putative signal peptide could be translocated into microsomes, confirming its ability to act as a signal peptide (*50*). Thus, hydrophobic signal peptides may be the mechanism employed by the ricin, SLT-1, and ShT family of toxins for translocation to the cytosol.

REFERENCES

1. Merrit, E. A., and Hol, W. G. J. (1995) *Curr. Opin. Struct. Biol. 5*, 165−171.
2. Fraser, M. E., Chernaia, M. M., Kozlov, Y. V., and James M. N. G. (1994) *Nat. Struct. Biol. 1*, 59−64.
3. Garred, O., van Deurs, B., and Sandvig, K. (1995) *J. Biol. Chem. 270*, 10817−10821.
4. Garred, O., Dubinina, E., Holn, P. K., Olsnes, S., van Deurs, B., Kozlov, J. V., and Sandvig, K. (1995) *Exp. Cell. Res. 218*, 39−49.
5. Saleh, M. T., Ferguson, J., Boggs, J. M., and Gariépy, J. (1996) *Biochemistry 35*, 9325−9334.
6. Fringeli, U. P., and Günthard, H. H. (1981) in *Membrane Spectroscopy* (Grell, E., Ed.) pp 270−332, Springer-Verlag, Berlin.
7. Brauner, J. W., Mendelsohn, R., and Prendergast, F. G. (1987) *Biochemistry 26*, 8151−8158.
8. Ishiguro, R., Kimura, N., and Takahashi, S. (1993) *Biochemistry 32*, 9792−9797.
9. Oppenheimer, N. J. (1989) *Methods Enzymol. 176*, 78−89.
10. Cabiaux, V., Brasseur, R., Wattiez, R., Falmagne, P., Ruysschaert, J.-M., and Goormaghtigh, E. (1989) *J. Biol. Chem. 264*, 4928−4938.
11. Wang, X.-M., Mock, M., Ruysschaert, J.-M., and Cabiaux, V. (1996) *Biochemistry 35*, 14939−14946.
12. Harrick, N. J. (1967) *Internal Reflection Spectroscopy*, Interscience Publisher, New York.
13. Fraser, R. D., and MacRae, T. P. (1973) *Conformation in Fibrous Proteins and Related Synthetic Peptides*, pp 94−125, Academic Press, New York.
14. Frey, S., and Tamm, L. K (1991) *Biophys. J. 60*, 922−930.
15. Lafrance, C.-P., Nabet, A., Prud'homme, R. E., and Pézolet, M. (1995) *Can. J. Chem. 73*, 1497−1505.
16. Frushor, B. G., and Koenig, J. L. (1975) in *Advances in Infrared and Raman Spectroscopy* (Clark, R. J. H., and Hexter, R. E., Eds.) Vol. 1, pp 35−97, Haydon & Son, London.
17. Byler, M., and Susi, H. (1986) *Biopolymers 25*, 469−487.
18. Surewicz, W. K., Moscarello, M. A., and Mantsch, H. H. (1987) *J. Biol. Chem. 262*, 8598−8602.
19. Jackson, M., Mantsch, H. H., and Spencer, J. H. (1992) *Biochemistry 31*, 7289−7293.
20. Krimm, S., and Bandekar, J. (1986) *Adv. Protein Chem. 38*, 181−364.
21. Goormaghtigh, E., Cabiaux, V., and Ruysschaert, J. M. (1990) *Eur. J. Biochem. 193*, 409−420.
22. Oberg, K., Chrunyk, B. A., Wetzel, R., and Fink, A. L. (1994) *Biochemistry 33*, 2628−2634.
23. Chirgadze, Y. N., Shestopalov, B. V., and Yu, S. (1973) *Biopolymers 12*, 1337−1351.
24. Chou,Y. P., and Fasman, G. D. (1974) *Biochemistry 13*, 222−245.
25. Watts, A., Harlos, K., Maschke, W., and Marsh, D. (1978) *Biochim. Biophys. Acta 510*, 63−74.
26. Casal, H. L., Kohler, U., and Mantsch, H. H. (1988) *Biochim. Biophys. Acta 957*, 11−20.
27. Thomas, L. C., and Chittenden, R. A. (1970) *Spectrochim. Acta 26*, 781−800.
28. Nabet, A., Boggs, J. M., and Pézolet, M. (1994) *Biochemistry 33*, 14792−14798.
29. Subirade, M., Gueguen, J., and Pézolet, M. (1994) *Biochim. Biophys. Acta 1205*, 239−247.
30. Lee, D. C., Hayward, J. A., Restall, J. C., and Chapman. D. (1985) *Biochemistry 24*, 4364−4373.
31. Surewicz, W. K., and Mantsch, H. H. (1988) *Biochim. Biophys. Acta 952*, 115−130.
32. Pézolet, M., Bonenfant, S., Dousseau, F., and Papineau, Y (1992) *FEBS Lett.* 299, 247−250.
33. Susi, H., Timasheff, S. N., and Stevens, L. (1967) *J. Biol. Chem. 242*, 5460−5466.
34. Haris, P. I., Lee, D. C., and Chapman, D. (1986) *Biochim. Biophys. Acta 874*, 255−265.
35. Jackson, M., Haris, P. I., and Chapman, D. (1989) *Biochim. Biophys. Acta 998*, 75−79.
36. Mendelsohn, R., and Mantsch, H. (1986) *Prog. Protein−Lipid Interact. 2*, 103.
37. Braiman, M. S., and Rothschild, K. J. (1988) *Annu. Rev. Biophys. 17*, 541−570.
38. Tamm, L. K., and Talulian, S. A. (1993) *Biochemistry 32*, 7720−7726.
39. Hübner, W., and Mantsch, H. H. (1991) *Biophys. J. 59*, 1261−1272.
40. Nabedryk, E., Gringold, M. P., and Breton, J. (1982) *Biophys. J. 38*, 243−249.
41. Rothschild, K. J., Sanches, R., Hsiao, T. L., and Clark, N. A. (1980) *Biophys. J. 31*, 53−65.
42. Zhang, Y.-P., Lewis, R. N. A. H., Hodges, R. S., and McElhaney, R. N. (1992) *Biochemistry 31*, 11579−11588.
43. Huang, H. W., and Wu, Y. (1991) *Biophys. J. 60*, 1079−1087.
44. Montecucco, C., Papini, E., and Schiavo, G. (1991) in *Sourcebook of Bacterial Protein Toxins* (Alouf, J. E., and Free, J. E., Eds.) pp 45−56, Academic Press, London.
45. London, E. (1992) *Biochim. Biophys. Acta 1113*, 25−51.
46. Saleh, M. T. (1997) Ph.D. Thesis, University of Toronto.
47. Sandvig, K., Olsnes, S., Brown, J. E., Petersen, O. W., and van Deurs, B. (1989) *J. Cell Biol. 108*, 1331−1343.
48. Argent, R. H., Roberts, L. M., Wales, R., Robertus, J. D., and Lord, J. M. (1994) *J. Biol. Chem. 269*, 25705−26710.
49. Simpson, J. C., Lord, J. M., and Roberts, L. M. (1995) *Eur. J. Biochem. 232*, 458−463.
50. Chaddock, J. A., Roberts, L. M., Jungnickel, B., and Lord, J. M. (1995) *Biochem. Biophys. Res. Commun. 217*, 68−73.

BI970944+